

# Parallel Generation of L-Systems

Markus Lipp\* Peter Wonka† Michael Wimmer\*

\*Vienna University of Technology †Arizona State University  
Email: \*{lipp,wimmer}@cg.tuwien.ac.at, †pwonka@gmail.com

## Abstract

This paper introduces a solution to compute L-systems on parallel architectures like GPUs and multi-core CPUs. Our solution can split the derivation of the L-system as well as the interpretation and geometry generation into thousands of threads running in parallel. We introduce a highly parallel algorithm for L-system evaluation that works on arbitrary L-systems, including parametric productions, context sensitive productions, stochastic production selection, and productions with side effects. Further we directly interpret the productions defined in plain-text, without requiring any compilation or transformation step (e.g., into shaders). Our algorithm is efficient in the sense that it requires no explicit inter-thread communication or atomic operations, and is thus completely lock free.

## 1 Introduction

Procedural modeling techniques to compute large and detailed 3D models have become very popular in recent years. This leads to the question of how to handle the increasing memory requirements for such models. The current trend is towards data amplification directly on the GPU, for example tessellation of curved surfaces specified by a few control points. This results in low storage costs and allows generating the complex model only when needed (i.e., when it is visible), while also reducing memory transfer overheads. In the same vein, grammars can be viewed not only as a modeling tool, but also as a method for data amplification since a very short grammar description leads to a detailed model.

In this paper we investigate whether it is possible to efficiently evaluate one of the most classical procedural modeling primitives, L-systems, directly on parallel architectures, exemplified by current GPUs and multi-core CPUs. The main motivation is to

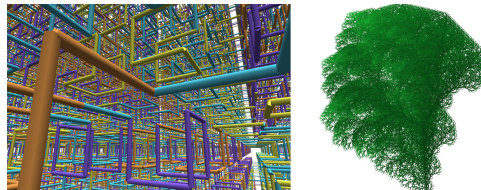


Figure 1: L-systems generated in real-time, at up to 198,000 modules per millisecond: Hilbert 3D space-filling curve and 2D plant.

enable interactive editing of large L-systems (examples are shown in Figure 1) by designers, therefore it is important to speed up the computation of L-systems in order to achieve low response times.

Although L-systems are parallel rewriting systems, derivation through rewriting leads to very uneven workloads. Furthermore, the interpretation of an L-system is an inherently serial process. Thus, L-systems are not straightforwardly amenable to parallel implementation. Previous work has therefore focused on specialized types of L-systems that do not allow side effects in productions, which makes them very similar to scene graphs [2]. In contrast, we deal directly with uneven workloads in L-system derivation, and we have identified two main sources of parallelism in the interpretation of L-systems: (1) the *associativity* of traversal in non-branching L-systems, and (2) the *branching structure* itself in branching L-systems.

The main contribution of this paper is a highly parallel algorithm for L-system evaluation that

- works on arbitrary L-systems, including parametric productions, context sensitive productions, stochastic production selection, and productions with side effects
- works directly on an input string and a plain-text representation of the productions without requiring any compilation or transformation

step (e.g., into shaders)

- is efficient in the sense that it requires no explicit inter-thread communication or atomic operations, and is thus completely lock free

To our knowledge, this is the first L-system algorithm that is highly parallel, i.e. utilizes thousands of threads in an efficient manner. This is achieved by identifying and exploiting the parallelism inherent in L-system derivation using parallel programming primitives like scanning or work-queue management, and a novel algorithm to explicitly resolve the branching structure. We demonstrate that our algorithm outperforms a well optimized single-core CPU implementation on larger L-systems.

**Overview:** First we will provide a background on L-systems and parallel primitives in Section 2. An analysis of the intrinsic parallelism of L-systems is provided in Section 3. Then our system consisting of two major building blocks will be described: (1) The derivation step will start with the axiom and generate a long string of modules (Section 4). (2) The interpretation step takes the string as input and generates the actual geometry (Section 5).

## 1.1 Previous Work

**General L-Systems:** Prusinkiewicz and Lindenmayer cover the basic L-system algorithm [7]. Multiple extensions to the basic approach were introduced [8, 9, 5].

**Parallelizing L-Systems:** Lacz and Hart showed how to use manually written vertex and pixel shaders combined with a render-to-texture loop to compute L-systems [2]. This concept was later extended using automatically generated geometry shaders [4]. Both methods require a shader compilation step for the productions. Further a transformation step of every production’s successor to a set of successors is needed to allow independent parallel executions in a shader. For example, the production  $L \rightarrow aLf[+L]Lf[-L]L$  is transformed to the set  $L \rightarrow aL, af + L, afL, aff - L, aff - L, affL$  [2]. This is only valid if the successor of  $L$  does not have any effect on the traversal state, which is not generally the case.

An algorithm utilizing multiple processors (the results show up to 8 CPUs) with distributed memory, communicating using the Message Passing Interface (MPI) was introduced [12]. In their algorithm, the derivation of the L-system is performed

using two binary trees, a Growth-State Tree (GST) and a Growth-Manner Tree (GMT). To actually render the system, the GST is interpreted as a scene graph. In order to get global scene-graph transformation matrices for rendering in the individual threads, the matrices are serially transferred from one process to the next.

**Parallel Computation in CUDA:** In order to access the parallel computing capabilities of GPUs we employ the NVIDIA CUDA data-parallel programming framework [1]. Recent work shows how to map computations having a highly dynamic nature to CUDA. Most notably, algorithms to efficiently implement workload balancing using a compactation step were introduced in the context of KD-trees [13], Reyes-style subdivision [6] and bounding volume hierarchies construction [3]. In the context of tessellating parametric surfaces, scan operations were used in order to scatter dynamically generated vertices to a VBO [10]. We employ both work-load balancing and vertex scattering in our work.

## 2 Background

Our work is based on L-systems and parallel processing primitives. Both concepts will be explained in this section.

**L-Systems** In our work, we use the formalism of parametric L-systems as introduced by Prusinkiewicz and Lindenmayer [7]. Parametric L-systems operate on *parametric words*, which are strings of *modules* consisting of *letters* with associated *actual parameters*. An L-system consists of a parametric word  $\omega$  called the *axiom*, and a set of productions describing how the current word is transformed. A production consists of a letter called the *predecessor* and a *successor*. The successor consists of a list of letters, where each letter can have multiple *arithmetic expressions* containing formal parameters. The predecessor can also consist of several letters, in which case the L-system is called context sensitive [7].

To actually generate geometry, two distinct phases are performed: A *derivation* phase generating a string of modules, and an *interpretation* phase in which the string of modules is interpreted in order to generate geometry.

**Derivation:** The derivation starts from the axiom. For every module contained in the axiom,

a *matching* production is searched. A production matches a module  $m$  if the letter of the predecessor matches the module letter. We then *apply* the matching production to the module: First, for every module in the successor, we calculate the actual real-valued parameters from the arithmetic expression. Then we *rewrite* the module  $m$  with the modules of the successor. One *iteration* consists in rewriting all modules in the string *in parallel* using matching productions [7].

**Interpretation:** The interpretation is performed *serially* from the start of the string, performing modifications of a *turtle state* based on predefined *turtle commands* associated with specific letters [7]. The turtle state represents the position and orientation of a virtual turtle. This state can be represented with a 4x4 matrix. The turtle commands associated to letters modify the turtle state, for example 'F' moves the turtle forward while drawing a line, or '+' rotates the turtle. Most of these turtle commands can also be expressed by a 4x4 matrix. A notable exception are the commands '[' and ']', which push and pop the turtle state on a stack, allowing the creation of *branching* (also called *bracketed*) L-systems [7].

**Parallel Primitives** We extensively use the parallel *scan* primitive in our work. Given an ordered set of values  $[a_0, a_1, \dots, a_n]$  and an associative operator  $\circ$  with the identity element  $I$ , an exclusive scan operation will result in the ordered set  $[I, a_0, a_0 \circ a_1, \dots, a_0 \circ a_1 \circ \dots \circ a_{n-1}]$  [11]. Unless noted otherwise, we always refer to an exclusive scan on integral values using the addition operator when we use the term scan in our work.

## 3 Analysis of Parallelism in L-System

### 3.1 Derivation

As an L-system is by definition a module string rewriting system utilizing *parallel* module replacements, the domain of parallelization is obvious: We simply assign chunks of the modules uniformly to multiple threads and perform the rewriting in parallel. The rewritings themselves are independent and thus do not need inter-thread communication. However, the output strings need to be concatenated again, which creates a dependency between the threads. The major problem here is that the length

of these strings can vary greatly: for a chunk containing  $n$  modules, the minimum expanded module amount is  $n$ . This case occurs when no production can be applied and thus every module is copied unmodified to the output. However, the maximum amount of modules is  $m^n$ , when the production with the maximum amount  $m$  of modules in the successor gets applied to each module.

Therefore, a parallel implementation has to efficiently cope with highly incoherent output module counts for each chunk. Previous shader-based approaches rely on the graphics pipeline to handle concatenation by load balancing (i.e. different output sizes of the geometry shader), which is not ideal because it can lead to serialization, and only works for special types of L-systems. In chapter 4 we show a native parallel solution to this problem utilizing the scan primitive.

### 3.2 Interpretation

The interpretation of a derived word is defined in a serial manner: Starting with an initial turtle state from the beginning of the module string, the position in the module string is advanced one by one, while applying a modification to the turtle state as defined by the letter of the current module. Therefore, the turtle state of every module string position is dependent on all previous turtle states. While it may look like there is no parallelism to exploit here, there are two inherent parallel concepts that can be extracted, as shown next.

**Associative Operations:** As mentioned before, most turtle commands and the turtle state can be represented as 4x4 matrices, except the push and pop commands. Further, as 4x4 matrix transformations can be combined, we can represent the turtle state up to a specific module string position using one matrix. The key point to parallelize the interpretation is to exploit the *associativity* of those matrix multiplications by accumulating matrices in each parallel chunk locally and combining them in a separate pass using a scan operation, as described in Section 5.1.

**Inherent Branch Hierarchy:** Since push and pop commands cannot be represented as matrices, the matrix approach cannot be applied for branching L-systems. Fortunately, the push/pop commands create another type of implicit parallelism that we can exploit: Every time a module representing a push command is encountered, two indepen-

dent interpretation branches are possible: the module string directly following the push command, and the module string following the corresponding pop command. Thus we can split the work at this point into two threads, as shown in Section 5.2.

## 4 Parallel Derivation

First we show how productions and module strings are efficiently represented on the GPU. Then we introduce the algorithm to perform one iteration of the derivation.

### 4.1 Efficient L-system Representations

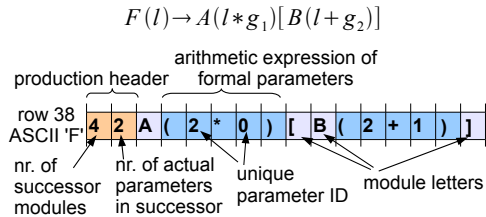


Figure 2: An example production of a parametric L-system packed in a texture.

In order to allow fast and efficient access to the productions, we store them in a 2D texture in the GPU version. For the multi-core CPU version we use a 2D array. The successor is stored in the row indexed by the ASCII-value of the predecessor’s letter. To resolve collisions of two productions that have the same predecessor letter, we create collision chains similar to hash tables.

We perform two simple optimizations: First, we count the number of modules and parameters occurring in the successor for later reference. Those values are stored in a designated header area. Second, in order to allow  $O(1)$  parameter value lookup during the derivation, we translate every parameter to a unique numerical ID. This process is visualized for parametric L-systems in Figure 2. In order to store stochastic or context sensitive productions, we extend the header area accordingly, by adding the production probability or respectively the left and right context letters.

**Representing the Module String:** A module string contains  $n$  module letters. As every module may have an arbitrary amount of parameters as-

signed, we use an additional array of size  $n$  containing indices to an array of actual parameters Figure 3 visualizes one module string.

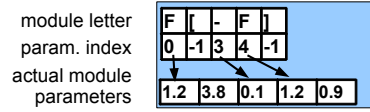


Figure 3: A module string represents a specific state during derivation. We store it as an array of module letters, a parameter index and the actual parameters.

### 4.2 Derivation

First, we prepare the axiom module string on the CPU side. In the GPU version we then upload it to the GPU. This step is extremely fast, as the axiom usually consists of just a few modules. For the desired iteration amount, we perform one iteration after the other on the GPU or the multi-core CPU. One iteration of the derivation takes the current module string as input and creates an expanded output module string.

The method to compute one iteration in parallel consists of three passes (or “kernels” of the parallel programming language) (see Figure 4):

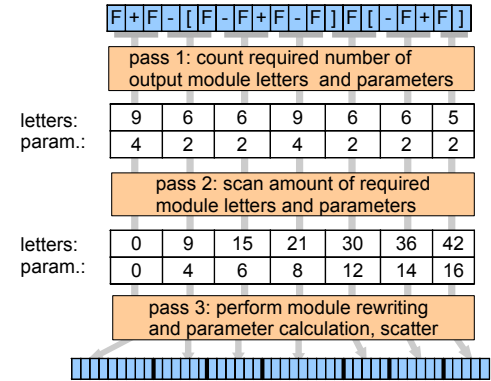


Figure 4: Three passes are performed during each iteration, transforming an input module string to an output module string. For better readability, we show only the letters of the input modules, and omit the parameters.

1. *Count.* We launch a kernel with  $n$  threads.  $m = \text{inputSize}/n$  subsequent modules from the

input module string are assigned to each thread. Each thread visits all  $m$  assigned modules, and fetches the amounts of required output module letters and parameters from the header section of the corresponding production. Those amounts are accumulated for all assigned modules, and finally written to an array in global memory.

2. *Scan*. We perform a sum-scan operation on this array, in order to calculate offset positions for the scattering of the result.

3. *Rewrite*. Again,  $m$  threads are launched, but this time the module replacement and parameter calculation is actually performed. This is done by fetching for each assigned module the matching production. If a production is *context-sensitive*, we also compare the left and right module letters of a module with the letters stored in the production header in order to determine if the production is applicable. For *bracketed context sensitive* L-systems the context search is more involved, as we need to take the push and pop commands into account. Therefore, for those systems, we perform a parallel hierarchy extraction step as explained in Section 5.2 before we start one iteration. For *stochastic* productions, we determine a random value for every applicable production, using a texture containing random values indexed by the position in the module string. This value is multiplied with the probability stored in the rule header. We then choose the rule with the highest result of the multiplication.

After having decided which production to use, we evaluate the parameters for every module in the production’s successor, and insert the resulting successor modules into the result module string. The parameter evaluation is conducted by a simple mathematical expression parser in the kernel. When no production is defined for a module, we simply copy it unmodified to the output. As we have the offset values to index the module string, every thread can write its resulting modules without interference from the other threads.

## 5 Parallel Interpretation

The result of a derivation is a module string. This needs to be converted into a geometric representation. There are two cases allowing two different parallel algorithms: non-branching and branching L-systems.

### 5.1 Non-Branching Module Strings

As explained in Section 3, most modules can be represented as associative matrix transformations. We can exploit this efficiently to interpret non-branching L-systems by interpreting chunks independently. We present a three pass algorithm (see Figure 5):

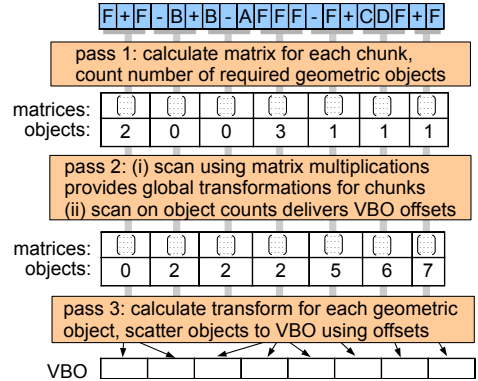


Figure 5: By exploiting the associativity of modules representable as matrix operations, we can efficiently interpret non-branching L-systems with this algorithm.

1. *Matrix accumulation* The string is split into  $m$  chunks, each chunk is assigned to an independent thread. In each chunk, we combine the matrices corresponding to the modules in the chunk, resulting in one local transformation matrix. Further, we count the amount of geometry generated in the modules. Both values are stored in an global array.

2. *Matrix scan*. A parallel scan operation is performed on the matrices, using  $4 \times 4$  matrix multiplication as the operator. The resulting array contains matrices representing a global transformation of the turtle state to the start of each chunk. Additionally, a scan using integer additions on the objects array is performed to calculate offsets for the geometry to be created.

3. *Geometry generation*. Finally, to get the global positions of each geometry object, we again operate on  $m$  chunks in parallel as in 1. and accumulate module matrices. But this time we do not start with the identity matrix but with the matrix determined during the scan. Furthermore, every time we encounter a geometry generation module, we calculate the global position of the object and in-

sert it into a vertex buffer object (VBO), using the offsets determined during the object scan.

The idea to use a scan to determine VBO offsets for tessellating parametric surfaces was introduced by Schwarz and Stamminger [10].

## 5.2 Branching Module Strings

For branching L-systems, parallelization is achieved by exploiting the branch hierarchy. Whenever a push command opening a new branch is encountered, two independent new work items are generated: one for the branch and one for the remaining string following the corresponding pop command. The main problem is to find the pop command in an efficient (i.e., parallel) way. This information is also necessary for fast context search in bracketed context sensitive systems. We therefore first present a novel parallel algorithm to extract the hierarchy, and then show how the work items can be efficiently managed.

### 5.2.1 Parallel Hierarchy Extraction

One critical observation is that when looking only at a particular hierarchy depth in the branch hierarchy, corresponding push/pop pairs follow each other directly. The main idea is therefore to extract the push and pop commands from the module string and sort their positions into buckets according to their depths. Each bucket will then contain the positions of corresponding push/pop pairs. These can then be easily traversed to store with each push the position of the corresponding pop.

We introduce an efficient parallel algorithm based on this idea that does not require direct communication between the blocks. We assume that we know the maximum depth of  $d_{max}$  of the branching hierarchy and allocate a two-dimensional bucket sort array with  $d_{max}$  rows. The complete algorithm is visualized in Figure 6, and consists of 5 passes operating on uniform chunks in parallel:

1. *Chunk depth calculation.* Starting at zero, we add 1 for every push, and subtract 1 for every pop occurring in a chunk. This results in the depth of the chunk end relative to the chunk start.

2. *Depth scan.* Performing a scan of those values results in the absolute depths of the start of each chunk.

3. *Depth-based push/pop count.* Now, by starting at the calculated absolute depth of the chunk start,

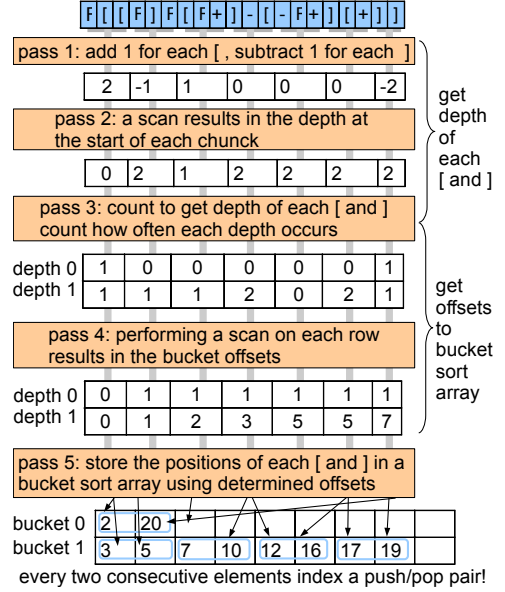


Figure 6: This algorithm allows efficient and parallel searching for corresponding push and pop pairs.

we can determine the absolute depth of every push and pop occurring in the chunk. We use this to determine the offsets for the bucket sort array by counting the amount of push and pop commands  $m_i$  in each depth  $j$  in the following way:  $c_j = \sum m_i \mid d_i = j$ . We store the values for  $c_j \mid 0 < j < d_{max}$  in a global array.

4. *Scan push/pop counts.* The scan of the  $c_j$  arrays results in the bucket offsets  $o_j$  each thread has to use in order to allow conflict-free writing to buckets.

5. *Write push/pop locations.* Again, we visit every push and pop command  $m_i$  of every chunk. But this time we write the absolute input module string position of the module  $m_i$  in the bucket  $d_i$  using the offset positions determined previously. This ultimately leads to a bucket sort array where every two consecutive elements in a row correspond to a push and pop pair.

Analogously to the matrix interpretation algorithm, we also calculate VBO offsets needed to scatter the geometry. In our implementation, this process is combined with pass 1, and the VBO offsets are stored as a parameter of push commands.

**Memory Footprint:** In order to reduce the memory footprint of the bucket sort array, we actually

use a one-dimensional array instead of two dimensions. This allows us to pack the bucket arrays for the individual depths without empty spaces tightly together. In the worst case, when every module in the module string is a push or pop module, the number of required memory elements is then equal to the amount of modules. The offsets needed for the 2D to 1D packing can simply be calculated from the values obtained in iteration 4:  $c_j + o_j$  of the last chunk equals the total amount of elements in a specific bucket. When we perform a scan operation of those values for each bucket we get the offsets to map the 2D bucket arrays into a 1D array.

**Integration into Module String:** As a last step, we use the information bucket arrays to write the position of corresponding push and pop modules directly into the module string to allow fast access during interpretation. This is a simple parallel algorithm: We evenly assign the 1D bucket array to multiple threads. Every even element in this array contains the position of a push command, every odd element references a pop command. Thus we need to write the position stored at every odd element as a parameter to the push module referenced by the preceding even element.

### 5.2.2 Work Queue-based Interpretation

As a result of the previously explained algorithm, every push module has a parameter indexing the position of the corresponding pop module, as well as a VBO offset parameter. With this information, we use a parallel work-queue approach [13, 3, 6]: One thread starts serially interpreting the module string. When a push-module is encountered, the thread creates two work items: One pointing to the module string following the push, and one pointing to the module string following the pop. The work items are then distributed to other threads using the previously introduced parallel methods [13, 3, 6].

## 6 Results

We implemented our parallel algorithms for GPUs utilizing CUDA and for multi-core CPUs using POSIX threads. In CUDA up to 1920 threads are utilized (60 blocks of 32 threads), the multi-core CPU version uses 4 threads. We compare those implementations against a highly optimized single-core CPU version. This version has the advantage

that no kernel or thread launch overheads occur, and that no scan or multi-pass operations are necessary. The test platform was an Intel Core 2 Quad Q6600 2.4GHZ PC with a Geforce GTX 280 graphics card.

L-system	bracketed	parametric	stochastic	context sens.
Hilbert 3D, pg. 20				
Koch curve, pg. 10 (d)				
row of trees, pg. 48		✓		
2D plant, pg. 25 (c)	✓			
3D tree, pg. 60 (b)	✓	✓		
plant stochastic, pg. 28	✓		✓	
p. ctx. sens., pg. 35 (b)	✓			✓

Table 1: Property matrix of the L-systems shown in our results. The page numbers refer to the L-system definitions by Prusinkiewicz and Lindenmayer [7].

**Test Scenes:** We used seven test scenes to demonstrate several aspects of our system. In order to ensure repeatability and comparability of our results, all our L-system productions are directly taken from Prusinkiewicz and Lindenmayer [7] for our performance measurements. In Table 1 we classify the test scenes according to the properties of the used production set.

**Rendering:** Our implementation creates a VBO containing lines. For our figures we use a geometry shader during rendering, creating cylinders from the lines. All our performance measurements do *not* contain the rendering times, as the rendering times are the same both for the CUDA and the CPU versions. Neither do the measurements contain the CPU-GPU memory transfer times required by the CPU versions, which we measured in the range from 20–40ms, making the CPU versions very hard to use in a real-time rendering setting.

**Scalability:** We evaluated how our derivation and interpretation scale with the number of iterations. For all our test scenes, we measured how long one specific iteration  $i$  of the derivation takes, and calculated the number of modules generated per microsecond during each iteration  $i$ . The results for three L-systems are shown in Figure 7. For the interpretation, a specific amount of derivation iterations was performed prior to the interpretation, the interpretation time was measured, and the amount

L-system, $i$	modules	total derivation times			total interpretation times			$d_f$	$i_f$
		ms	rel. speedup	CUDA	ms	rel. speedup	CUDA		
Hilbert 3D, 6	1,266,864	4.70	3.76	2.92	31.50	1.23	6.61	5	5
Koch curve, 7	915,049	3.45	3.26	3.20	22.56	0.70	2.99	6	6
row of trees, 10	815,545	10.21	3.29	3.15	77.04	4.25	10.84	8	7
2D plant, 7	813,169	3.31	3.04	3.15	22.45	1.27	1.21	6	7
3D tree, 16	622,334	8.53	1.40	1.17	31.44	2.78	3.87	13	13
plant stoch., 11	835,481	6.45	1.75	3.23	14.70	0.09	0.24	9	?
p. ctx. sens., 30	25,174	0.73	0.39	0.03	0.11	0.43	0.11	?	?

Table 2: Performance measurements.  $i$  shows the amount of iterations performed. The single-core CPU times are absolute values in milliseconds, the multi-core CPU and CUDA values are relative speedups compared to the single-core CPU values.  $d_f$  denotes the first iteration where CUDA is faster compared to the single-core CPU version during derivation,  $i_f$  is analogous for interpretation.

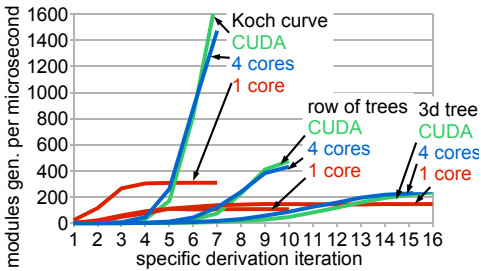


Figure 7: Scalability analysis of the derivation step. For every iteration, we calculate the number of modules generated per microsecond.

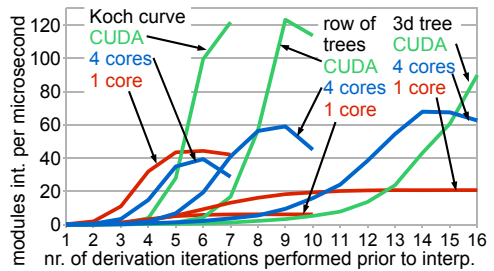


Figure 8: Scalability analysis of the interpretation step. We performed a specific amount of derivation steps before the interpretation was performed.

of modules interpreted per microsecond was calculated. The results are shown in Figure 8. For readability only three L-systems are shown, but all results show a similar pattern: As expected the initial iterations incur some overhead in the parallel implementation on the GPU and the multi-core CPU, because the amount of parallelism is limited, and the overhead of launching CUDA-kernels or POSIX threads is a significant factor. This makes parallel versions slower on the first few iterations. For the later iterations the parallel implementations are several times faster, because a high amount of threads can be utilized. For all L-systems, we list the first derivation iteration  $d_f$  where CUDA is faster compared to the single-core CPU version, as well as the first interpretation of a string generated with  $i_f$  iterations where CUDA is faster in Table 2. The total performance including the cases where CUDA is slower will be discussed in the next two paragraphs.

**Total Derivation Performance:** The CUDA and the multi-core CPU version are very similar in performance and are significantly faster than the single-core CPU version in most cases. There are two notable exceptions: First, the 3D tree is only marginally faster. Second, the context sensitive plant is considerably slower. Both cases can be attributed to the following observation: The corresponding L-systems are growing rather slowly, compared to the other test cases. For the 3D tree 622,334 modules are created in 16 iterations, while the plant creates only 25,174 modules in 30 iterations. All other tested L-systems create more modules with a lower iteration count. Therefore the other L-systems have less relative thread launch overhead. To sum it up, during the derivation the parallel implementations are significantly faster when the L-systems grow relatively fast. Another important thing to note is that the results for the

stochastic system vary with the random seed, our measurements were in a range of about +/- 20% for different seeds.

**Total Interpretation Performance:** The three tested non-bracketed (serial) L-systems are significantly faster in CUDA compared to the other versions, probably because the parallel matrix interpretation makes good use of the high arithmetic density of the GPU. On the other hand, the multi-core CPU version performs rather bad on those L-systems (with the exception of the row of trees L-system), probably the matrix multiplications and the memory bandwidth are the limiting factors here.

The results for the branching L-systems vary. The first thing to note is that the five-pass hierarchy extraction step requires considerably less time than the actual interpretation. For reference, a hierarchy extraction takes 3.3ms on one CPU core and 1.97ms in CUDA for the 2D plant. Our interpretation of the varying results is that the L-systems have different branching structures, which directly affect how effective our work-queue interpretation is: The 3D tree (Figure 9) has very regular branching, and is considerably faster to interpret with the parallel versions, while the 2D plant (Figure 1) exhibits more irregular branching, resulting in only a small speedup. The stochastic plant contains only a few long branches with many small ones attached (Figure 9), making it hard to spread the work to multiple threads. The context sensitive plant is even harder for the parallel algorithms to interpret, as the amount of modules is very low compared to the other cases. In summary, the non-bracketed L-systems are considerably faster in CUDA, while the bracketed L-systems create varied results based on the branching structure.

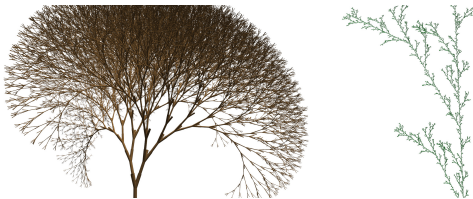


Figure 9: L-systems generated in real-time: 3D tree and stochastic plant.

## 7 Discussion

**Comparison to Previous Work:** The main advantage over the previous GPU-based methods [2, 4] is that we make explicit use of parallel primitives and do not rely on the graphics pipeline to deal with data amplification and other issues. We fully support productions having side-effects and thus do not need to rely on the specific side effect-free turtle commands presented by Lacz and Hart [2]. Furthermore, we can directly use the productions without requiring a compilation or transformation step. Compared to the multi-CPU based method proposed by Yang et al. [12] our algorithm does not need an intermediate scene-graph representation of the module string. Furthermore our algorithm can utilize thousands of threads, which is significantly higher than what was shown in the multi-CPU version.

**Memory Transfer to Graphics Hardware:** One important advantage of our CUDA version is that the resulting geometry already resides in GPU memory, so there is no need for a copy operation. The CPU versions, on the other hand, needs to perform a copy from the main system memory to the GPU. We measured copy times of about 20–40ms for the tested L-systems – this is very high compared to the generation times, increasing the total speedup of CUDA significantly, and showing that a GPU implementation is highly desirable. All our results do *not* include those transfer times.

**Intra-Block Thread Divergence:** In CUDA, when different execution paths are taken within a sub-block of threads (called warp), those execution paths are serialized, reducing the utilization of the intrinsic SIMD capabilities. In our algorithm, the following situations lead to divergence in the code: (1) If two productions produce a successor of different length during derivation. This divergence is directly caused by the varying data amplification, and can probably not be avoided. (2) During interpretation, the matrix notation helps in maintaining thread coherence, as we can perform the multiplications coherently after each thread decides which matrix to use based on the associated commands. However, when some threads either have no command to perform or have a geometry generation command, SIMD can not be fully utilized. (3) The length of one work item can vary, leading to divergence. Unless we would further split work items into sub work

items, we can probably not avoid this divergence.

**Limitations:** The varying results of the work-queue approach indicate that there may be future work necessary in creating more consistent speedups, maybe a more elaborate work-queue management can achieve this. As for the tested context sensitive L-system, the high iteration counts result in a low performance of the CUDA approach, making the use of the CPU version more appropriate in this case.

## 8 Conclusion

In his paper we introduced a solution to generate L-systems on a parallel architecture. We make two major contributions. First, we show how parallel primitives can be employed to handle the varying data amplification during derivation. Second, we introduce an algorithm to match the push and pop stack operations to obtain a parallel implementation of L-system interpretation. The system can work with a broad set of rules, including parametric rules, stochastic rules, and context-sensitive rules. We have demonstrated that our parallel L-system outperforms a highly optimized single-core CPU implementation in many test cases, while there are some cases where the a single-core version is faster. The advantage of our GPU version gets more pronounced when taking into account CPU-GPU memory transfer times required by the CPU versions.

**Future Work:** We would like to integrate the parallel derivation of L-systems in a rendering engine to render large-scale environments. We plan to combine the derivation of L-systems with occlusion queries and memory management algorithms so that we can render environments several times the size of graphics card memory in real time. Also, it would be interesting to extend the work to procedurally generated architecture, and more complex L-system concepts.

**Acknowledgements:** This research was supported by the Austrian FIT-IT Visual Computing initiative, project GAMEWORLD (no. 813387), and by the NSF, contract nos. IIS 0612269, CCF 0643822, and IIS 0757623.

## References

[1] NVIDIA CORPORATION. Cuda: Compute unified device architecture.

<http://developer.nvidia.com/>. 2007.

[2] P. Lacz and J.C. Hart. Procedural geometry synthesis on the gpu. In *Workshop on General Purpose Computing on Graphics Processors*, pages 23–23, NY, USA, 2004. ACM.

[3] C. Lauterbach, M. Garland, S. Sengupta, D. Luebke, and D. Manocha. Fast bvh construction on gpus. *Computer Graphics Forum*, 28(2):375–384, 2009.

[4] M. Magdics. Real-time generation of l-system scene models for rendering and interaction. In *Spring Conf. on Computer Graphics*, pages 77–84. Comenius Univ., 2009.

[5] Y.I.H. Parish and P. Müller. Procedural modeling of cities. In *SIGGRAPH '01*, pages 301–308, NY, USA, 2001. ACM.

[6] A. Patney and J.D. Owens. Real-time reyes-style adaptive surface subdivision. *ACM Trans. Graph.*, 27(5):1–8, 2008.

[7] P. Prusinkiewicz and A. Lindenmayer. *The algorithmic beauty of plants*. Springer-Verlag, Inc., NY, USA, 1990.

[8] P. Prusinkiewicz, M.J., and Radomír Měch. Synthetic topiary. In *SIGGRAPH '94*, pages 351–358, NY, USA, 1994. ACM.

[9] P. Prusinkiewicz, L. Mündermann, R. Karwowski, and B. Lane. The use of positional information in the modeling of plants. In *SIGGRAPH '01*, pages 289–300, NY, USA, 2001. ACM.

[10] M. Schwarz and M. Stamminger. Fast gpu-based adaptive tessellation with cuda. *Computer Graphics Forum*, 28(2):365–374, 2009.

[11] Shubhabrata Sengupta, Mark Harris, Yao Zhang, and John D. Owens. Scan primitives for gpu computing. In *Graphics Hardware*, pages 97–106, NY, USA, 2007. ACM.

[12] T. Yang, Z. Huang, X. Lin, J. Chen, and J. Ni. A parallel algorithm for binary-tree-based string rewriting in l-system. In *Proc. of the Second International Multi-symposiums of Computer and Computational Sciences*, pages 245–252, Los Alamitos, California, 2007. IEEE Computer Society Press.

[13] K. Zhou, Q. Hou, R. Wang, and B. Guo. Real-time kd-tree construction on graphics hardware. *ACM Trans. Graph.*, 27(5):1–11, 2008.